Does the Build Orientation Parameter Affect the Fit of Fixed Partial Dentures Fabricated by Additive Manufacturing?

Elie E. Daou, DDS, DESP, MSc, PhD

Department of Prosthodontics, Faculty of Dental Medicine, Lebanese University, Beirut, Lebanon; Department of Fixed Prosthodontics, Faculty of Dental Medicine, Saint Joseph University, Beirut, Lebanon.

Purpose: This in vitro study evaluated the adaptation of cobalt-chromium (Co-Cr) fixed dental prostheses (FDPs) fabricated by selective laser melting (SLM) with different build angles. ***Materials and Methods:*** Maxillary right first premolars and first molars from a typodont were prepared with 1-mm chamfer, 2-mm occlusal reduction, and total taper of 8 degrees to receive three-unit FDPs. After framework design, data were sent to a laser machine, and 30 specimens were fabricated from Co-Cr metal powder by SLM. Specimens were assigned to three groups (n = 10 per group) with different build angles of 0 (A0), 30 (A30), and 45 (A45) degrees. Marginal and internal fit were evaluated. Results were compared among build orientation groups and abutments. Data were analyzed using the Levene test, *t* test, and analysis of variance (α = .05). ***Results:*** A statistical difference was found between different angle groups (P = .015). At the abutment level, a significant difference was found in the gap values between build orientation groups for the molars (P = .048). Group A0 reported the smallest mean discrepancy values, and group A45 the highest. Statistical differences were found between group A45 and groups A0 (P < .001) and A30 (P < .024). ***Conclusions:*** The fit of printed metal FDPs was affected by the build orientation but remained clinically acceptable.
Int J Prosthodont 2024;37(suppl):s41–s47. doi: 10.11607/ijp.8343

Compared to the conventional lost-wax technique, CAD/CAM systems are less dependent on the dental technician's skills and have fewer operator procedures and reduced processing time and production costs.[1–5] CAM systems include subtractive milling and additive manufacturing (AM). The most commonly used additive technology to produce cobalt-chromium (Co-Cr) and titanium alloys structures is the powder bed fusion technology, which includes selective laser sintering, selective laser melting (SLM), and electron beam melting.[6]

In the SLM process, the piece is built following a build direction, fixed as the z axis. The process starts by slicing the 3D CAD design in a 2D contour in the x-y plan at each level of the build axis. From this 2D contour, a slice thickness is added cumulatively at the successive slicing plans.[7] A laser is scanned on metal powders (particle size: 20 to 60 µm) to generate a layer of products following the sliced data.[8] The alloy powders are completely melted using CO_2 or Nd:YAG lasers in argon or nitrogen inert chamber.[9] This sequence continues until the production

Correspondence to:
Elie E. Daou,
edaou@ul.edu.lb
elie.daou2@usj.edu.lb

Submitted May 19, 2022; accepted October 19, 2022.

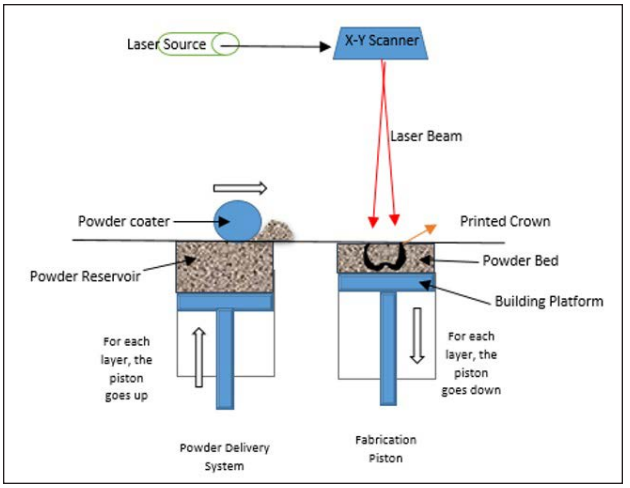

Fig 1 Schematic presentation of the selective laser melting process.

of a near-net-shape of the designed structure. Free-form shaping can be achieved without any mold and beyond the limitations of the cutting tools, allowing the fabrication of dental restorations with complex geometries.[10] Although reduced material waste and lightweight designs have been appreciated,[11–13] drawbacks like reduced construction framework scale, slow building speed, and uncertain dimensional precision have also been raised.[4] Moreover, construction design, process parameter settings, and postprocessing procedures need time and effort.[14,15] Many aspects of this technology (like part accuracy, processing cost, and product mechanical properties) remain challenging,[16] and variations in product characteristics are related to the process settings.[14,17–20] Major parameters—such as slice thickness, build axis, thermal errors, and support structures—can affect the object accuracy.[7]

Co-Cr alloys are preferred for the fabrication of metal frameworks because of their good biocompatibility and exceptional mechanical properties.[21] In fixed dental prosthesis (FDP) construction, an adequate adaptation is crucial for abutment preservation, periodontium health, and clinical longevity. A microleakage may occur from increased marginal discrepancy, leading to cement dissolution, secondary caries, bacterial growth, and periodontal disease.[22] Customized dental prostheses have been produced with a fit equivalent to that of traditional cast restorations.[22–25]

The key constraint in AM is achieving an accurate object. The build direction, which is an important AM parameter to be set before the manufacturing start, will affect the tolerated errors, consumed energy, and needed volume of support structures,[26] with differences in the final product properties.[16] The building orientation influences the printing time resulting from variations in the number of layers between the selected directions.[27] The chosen build angle should require the least number of support structures with minimal finishing and polishing time.[28] The shrinkage between layers is also dependent on the build orientation,[29] influencing the mechanical properties of the final product.[30] Limited data have been provided regarding the adaptation of vat photopolymerized products,[31–33] but not in SLM metal FDP manufacturing. Thus, the objective of this in vitro study was to evaluate the influence of build orientation parameter on the fit of Co-Cr multi-unit prostheses fabricated by AM. The null hypotheses were: *(1)* the different build angles would not lead to prostheses fit difference; and *(2)* the adaptation would be related to the abutment preparation.

MATERIALS AND METHODS

The maxillary right first premolar and first molar from a typodont model (A3, Frasaco) were prepared to receive three-unit FDPs, with a 360-degree 1-mm chamfer, 2-mm occlusal reduction, and 8 degrees total taper.[34] The dies were scanned with a scanner (Ceramill Map 400, Amann Girrbach), and the framework design was done by using a software (Ceramill Mind, Amann Girrbach), setting the connector cross-section at 9 mm^2, the wall thickness at 0.6 mm, and the cement space at 30 µm at 1 mm above the margin.[15] The initial design was cut back to allow a ceramic layering of 1.5 mm. The data were transferred to a printing machine (SLM 100, ReaLizer) for specimen production via a metal powder (Mediloy S-Co, Bego). The printing parameters were set as follows: a scan speed of 7 meter/second, a focus diameter of 40 µm, a Yb-fiber laser power with a wavelength between 1,060 and 1,100 nm, a laser power output of 200 W, and a surface power density of 25 kW/mm^2 under nitrogen gas (Fig 1).[35–37] The same printing parameters were used for all 30 dies, but three different build angles were used (10 dies per angle group): build orientation of 0 degrees (group A0), build orientation of 30 degrees (group A30), and build orientation of 45 degrees (group A45). In the 0-degree frameworks, the FDP occlusal surface was parallel to the platform; whereas for the 30- or 45-degree frameworks, these surfaces were rotated by 30 or 45 degrees, respectively, along the prosthesis long axis (Fig 2).[31]

The internal residual stress of the frameworks was relieved using a furnace (LT 15/12/P330, Nabertherm) at 650°C. The temperature was increased to 800°C within a span of 12 minutes and held for 15 minutes, then cooled down within 15 minutes to 550°C. The specimens were removed for further processing when the temperature was below 550°C (Fig 3).[36]

The marginal and internal fit of frameworks was measured using the silicone replica technique.[31] A light-body silicone (Aquasil Ultra light, Dentsply Sirona) was applied

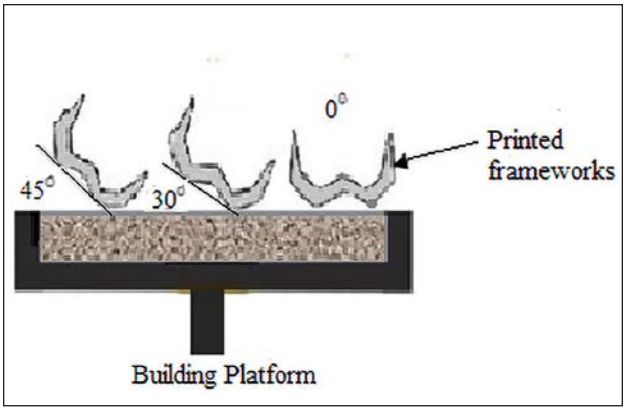

Fig 2 Schematic drawing of the designed frameworks with different build angles (0, 30, and 45 degrees) of the occlusal planes to the building platform plane.

Fig 3 A printed fixed partial denture fixed on its abutment model.

Table 1 Comparison Between Groups for Each Measured Location

	M1	M2	M3	M4	M5	M6	M7	M8	M9
Build angle groups									
A0	38 ± 5	59 ± 4	68 ± 4	128 ± 6	178 ± 8	156 ± 10	79 ± 4	70 ± 5	54 ± 5
A30	59 ± 5	56 ± 4	76 ± 4	136 ± 6	169 ± 8	166 ± 10	82 ± 4	87 ± 5	82 ± 5
A45	64 ± 5	70 ± 4	95 ± 4	160 ± 6	195 ± 8	160 ± 10	99 ± 4	82 ± 5	92 ± 5
P	.002	.083	.001	.012	.179	.824	.023	.128	< .001

A0 = 0-degree angle; A30 = 30-degree angle; A45 = 45-degree angle; M1–M9 = different measured locations.
Data are presented in μm as mean ± SD.

in the copings intaglio, which were directly placed on the metal die with a compression force of 40 N applied on the pontic central fossae.[38] After complete polymerization, the copings were removed with the adherent light body. A medium-body material (Aquasil Ultra medium, Dentsply Sirona) was then added to support the silicone light body. The replica process was redone when any flaw was found within the silicone film. The prepared silicone was segmented with a razor blade in the mesiodistal and buccolingual planes, at the central fossae deepest point, using a prepared acrylic resin guide (Unifast, GC).

One operator (E.E.D.) measured the discrepancies using a stereomicroscope (SZX-ZB7, Olympus) with a built-in measuring program. Measurements were performed on digital images at ×20 magnification. A total of 18 locations were measured (M1 to M9), in the mesiodistal and buccolingual planes for both abutments.[5] The marginal measurement value was considered as the mean of M1, M2, M8, and M9; the axial value as the mean of M3 and M7; and the occlusal value as the mean of M4, M5, and M6 in all planes. An intraclass correlation coefficient test of .969 was found.

A power analysis determined the sample size to be 8.98 at 99% power.[37] The discrepancy values between the materials and the abutments were compared using Levene test and *t* test (SPSS version 23.0, IBM). Analysis of variance and Bonferroni correction were used for multiple pairwise comparisons. Equality of variances was assessed with Levene test (α = .05 for all tests).

RESULTS

The difference between groups was statistically different (F = 4.367, df = 2, *P* = .015), but not between abutments (F = .632, df = 1, *P* = .428). The difference was significant among molars (F = 3.219, df = 2, *P* = .048), but not among premolars (F = 2.166, df = 2, *P* = .125), with a mean fit value of 108 ± 28 μm for the molars and of 104 ± 16 μm for the premolars (Table 1). The biggest mean gap was found in group A45, and the smallest gap in group A0 (Table 2). Statistical differences were reported between groups A0 and A45 (*P* < .001) and between groups A30 and A45 (*P* = .024) (Table 3). Figure 4 shows the estimated gap in means in the different measured regions and abutments.

Table 2 Estimated Mean Gaps from Build Angle Groups

			95% CI	
Build angle groups	Mean	SE	Lower	Upper
A0	92.6 µm	4.5 µm	83.5 µm	101.6 µm
A30	106.0 µm	3.7 µm	98.6 µm	113.4 µm
A45	112.4 µm	3.7 µm	105.0 µm	119.8 µm

A0 = 0-degree angle; A30 = 30-degree angle; A45 = 45-degree angle; SE = standard error.

Table 3 Multiple Pairwise Comparisons to Measure Gap for Techniques, Based on Observed Means

					95% CI	
Angle I	Angle J	Mean difference (I–J)	SE	*P*	Lower	Upper
A0	A30	–9.1 µm	4.1	.093	–17.1 µm	1.2 µm
A0	A45	–20.3 µm	5.3	< .001	–3.2 µm	–9.1 µm
A30	A45	–11.2 µm	4.2	.024	–12.1 µm	–1.3 µm

A0 = 0-degree angle; A30 = 30-degree angle; A45 = 45-degree angle.
The mean difference is significant at the .05 level.

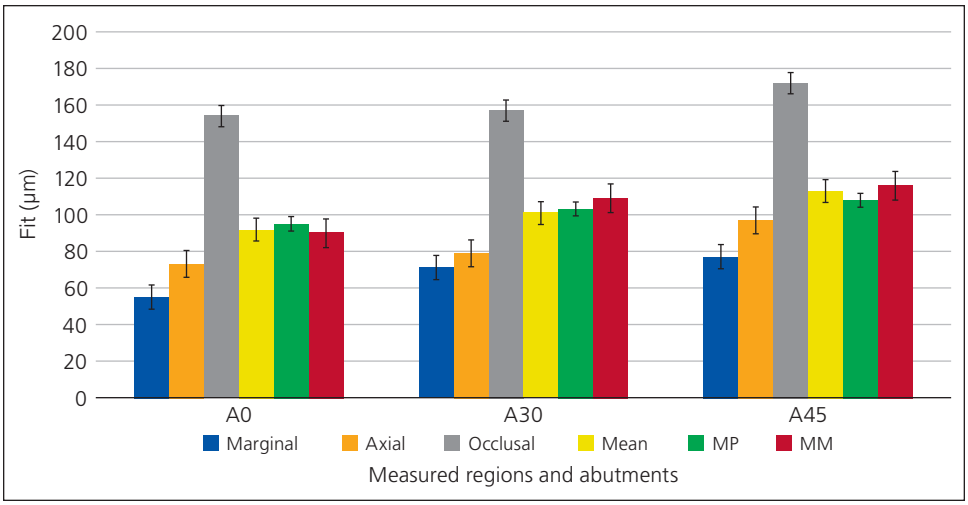

Fig 4 Comparison of fit between build-orientation groups in the different measured regions. A total of 18 measurements were performed on mesiodistal and buccolingual planes (9 measurements [M1–M9] per plane) for both abutments. Marginal = mean of M1, M2, M8, and M9; axial = mean of M3 and M7; occlusal = mean of M4, M5, and M6. A0 = 0-degree angle; A30 = 30-degree angle; A45 = 45-degree angle; MM = maxillary right first molar model; MP = maxillary right first premolar model.

DISCUSSION

The results of this study indicate that the metal framework fit was related to the build orientation, and thus the first null hypothesis was rejected. Authors have mainly evaluated the fit of FDP resin casting patterns with different build orientations.[27,31,39] The present findings are consistent with previous conclusions in printed provisional crowns where the 0-degree build orientation had the optimal fit.[31,32] Zero- and 30-degree build angles have been recommended for better marginal and internal fit,[32] but another study recommended 30 or 45 degrees.[39] These conclusions confirmed that the build angle influenced the structure characteristics,[32,39–42] with statistical differences in the marginal and internal fit and variations in build support, finishing, and polishing time and effort.[33,40]

The build orientations were chosen based on a previous study.[31] Comparison with other studies was difficult because the other authors have only worked on resin and casting patterns.[31,32,39] In the present study, the 45-degree build orientation produced discrepancies significantly greater than those of the other groups, which is consistent with other findings.[31,39] The marginal gaps generated by the three groups were clinically acceptable,[39] whereas in a previous study, only the 0-degree casting patterns had values < 120 µm.[31] Laser penetration may vary with build orientation.[41] In group A45,

during the construction of the buccal wall of the specimens, excessive polymerization may have occurred that necessitated a framework tilt during insertion.[31]

Several process parameters—including slice thickness, build orientation, support structures, and hatching pattern—have played a major role in the final product quality and accuracy.[7,43] Build orientation may help to overcome the limited build platform size and slow build rate and can reduce the postprocessing procedures.[4] The build angulation may be set manually or automatically using different algorithms,[44] taking into account the printing time and the amount and area of support.[45] In the AM process, normally the layer in construction is supported against gravity by the previously polymerized layer. Some regions of the newly deposited layer may be overexposed, presenting an overhang area opposite to the build direction. The gravity effects may induce a deformation of the overhanging walls and affect the marginal fit.[31] Different overhang areas may result from different build orientations, with additional support structures and increase in material quantity, build time, process cost, and surface quality deterioration in contact with support regions.[16] Attaching build structures increases the build time,[32] with the shortest time required for the 0-degree build orientation.[31] Depending on the geometry of the object, the surfaces forming an angle with the long axis between 0 and 30 degrees must be supported; whereas surfaces with bigger angles can be self-supported,[33] with a variation in dimension related to the support configuration.[40] In the 0- and 30-degree angles, the margins were supported; this can explain the significant difference found with the results of the 45-degree angle in the present study. If a 90-degree angle was considered, the opposite margins of the ones supported by the platform will be in an overhang position, where maximum deviations have been found.[33]

The surface roughness of the SLM products may be influenced by the building direction and the choice of support.[2] With the product's surface quality determined by the layer-by-layer apposition,[46] the metal powder–based process encounters several challenges, including trying to reduce the staircase effect with a poor surface finish and using minimal support structures for the overhanging regions.[7] Each layer addition results in complex time-dependent temperature profiles, with frequent thermal cycling affecting the material microstructure.[47] During the AM process, the upward-facing surfaces are totally exposed to the laser beam, and the heat can be dissipated through the layers underneath the top one.[2] Subsequently, the metal powders can be totally molten. For downward-facing surfaces touching the powder bed, an overheat occurs from the poor heat transfer of the unmelted powders. When the melt pool solidifies, the unmelted powders may adhere to the downward-facing surfaces, leading to a higher surface roughness.[48] Precipitates have been observed along the build direction. Increasing the inclination angle of the downward-facing surface may produce smoother external surfaces[49] but rougher internal surfaces. Throughout the SLM procedure, the remaining unmelted underlying metal powder is sintered to the AM object surface. Consequently, partially molted powder can be found on the metal surface. This can explain the higher gap values associated with increased build angle, where some of the crown's intaglio surface became downward-facing surfaces. Different volumetric errors and surface qualities may have resulted from different build directions with different stair stages.[7] It is still technologically impossible to overcome the volumetric error resulting from the mismatch between the nominal and real surfaces, with some deterioration in the surface quality.[50] Differences between a designed and final product have been also encountered due to several drawbacks like the stair-stepping effect.[16] Mechanical, chemical, sandblasting, machining, or laser polishing postprocessing procedures have been proposed to modify the object surface.[4,51]

Temperature fluctuations during production may lead to high internal tension, which alters the product accuracy.[52] A heat source is used to selectively melt material in the layer with the help of a scan strategy. This may induce alternative compressive and tensile stresses in the successive layers, with a complicated stress distribution related to temperature variations within the layer.[7] The residual stress distribution is correlated with the process parameters, the geometry of the printed object, and the building orientation. The latter will influence the stress distribution because of the changes in the boundary orientations. The 0-degree design, built with greater area in contact with the building platform, has resulted in lower residual stress levels.[53] A postprocessing heat treatment is needed to relieve the internal residual stress resulting from process thermal gradients.

The framework fit was not dependent on the abutment form, and thus the second null hypothesis was rejected. However, the adaptation differed among different locations on the molars, which is onsistent with other findings.[11,15,54] This difference has not been statistically significant in the marginal fit on premolars and molars.[55] Acquisition quality and digital data processing can affect the prosthesis fit.[25,55] A marginal gap of 120 µm has been considered clinically permissible,[56] but it can range between 100 and 150 µm.[57] The prosthesis retention and resistance may be affected by the internal fit,[58] whereas the occlusal gap is usually larger compared to the other measured areas.[59] A larger cement space would have overcome the small differences found among the prostheses adaptation.[31] The occlusal and incisal gaps have been 1.5× to 5× greater than the predefined cement space in 3D-printed interim crowns.[32,60,61] However, the axial gap acts differently, with values sometimes smaller

than the cement space.[61] Errors in standard tessellation language file splitting and pattern shrinkage have been blamed, with an imperfect fit necessitating increased cement space for better adaptation.[40,61]

Major sources of errors (such as container effect, staircase effect, overcure, tessellation, number of build layers, sharp corners, distortion, and shrinkage) during the AM build process have been acknowledged.[62,63] Build time, energy consumption, and material utilization may be considered proportional to the build height, taking into consideration the setting program.[16] A limitation of the present study was that only one dental alloy and one laser melting machine, with selective build angles, were used in the FDP fabrication. Additional research is needed to assess the effect of different parameters on the prostheses fit, where different results may be obtained. However, evaluating several parameters within the same study can make conclusions difficult.

CONCLUSIONS

Based on the findings of this in vitro study, the following conclusions were drawn:

1. The build direction affected the marginal and internal fit of the Co-Cr prostheses fabricated by SLM.
2. Clinically acceptable marginal fit was found for the different build orientations.
3. The prosthesis adaptation differed among different locations on the molars.

ACKNOWLEDGMENTS

The author declares no conflicts of interest.

REFERENCES

1. Sun J, Zhang FQ. The application of rapid prototyping in prosthodontics. J Prosthodont 2012;21:641–644.
2. Konieczny B, Szczesio-Wlodarczyk A, Sokolowski J, Bociong K. Challenges of Co-Cr Alloy additive manufacturing methods in dentistry—The current state of knowledge (systematic review). Materials (Basel) 2020;13:3524.
3. Bae E, Kim JH, Kim WC, Kim HY. Bond and fracture strength of metal-ceramic restorations formed by selective laser sintering. J Adv Prosthodont 2014;6:266–271.
4. Revilla-León M, Sadeghpour M, Özcan M. A review of the applications of additive manufacturing technologies used to fabricate metals in implant dentistry. J Prosthodont 2020;29:579–593.
5. Daou EE. Effect of ceramic layering on the fit of cobalt-chromium alloy 3-unit fixed dental prostheses fabricated by additive, soft milling, and casting technologies. J Prosthet Dent 2021;126:130.e1–e7.
6. Witkowski S. CAD/CAM in dental technology. Quintessence Dent Technol 2005;28:169–184.
7. Das P, Chandran R, Samant R, Anand S. Optimum part build orientation in additive manufacturing for minimizing part errors and support structures. Procedia Manufacturing 2015;1:343–354.
8. Tan XP, Tan YJ, Chow CSL, Tor SB, Yeong WY. Metallic powder-bed based 3D printing of cellular scaffolds for orthopedic implants: A state-of-the-art review on manufacturing, topological design, mechanical properties and biocompatibility. Mater Sci Eng C Mater Biol Appl 2017;76:1328–1343.
9. Murr L, Gaytan SM, Ramirez DA, et al. Metal fabrication by additive manufacturing using laser and electron beam melting technologies. J Mater Sci Technol 2012;28:1–14.
10. Takaichi A, Suyalatu, Nakamoto T, et al. Microstructures and mechanical properties of Co–29Cr–6Mo alloy fabricated by selective laser melting process for dental applications. J Mech Behav Biomed Mater 2013;21:67–76.
11. Kim SB, Kim NH, Kim JH, Moon HS. Evaluation of the fit of metal copings fabricated using stereolithography. J Prosthet Dent 2018;120:693–698.
12. Khaledi AA, Farzin M, Akhlaghian M, Pardis S, Mir N. Evaluation of the marginal fit of metal copings fabricated by using 3 different CAD-CAM techniques: Milling, stereolithography, and 3D wax printer. J Prosthet Dent 2020;124:81–86.
13. Sames WJ, List FA, Pannala S, Dehoff RR, Babu SS. The metallurgy and processing science of metal additive manufacturing. Int Mater Rev 2016;61:315–360.
14. Hesse H, Özcan M. A review on current additive manufacturing technologies and materials used for fabrication of metal-ceramic fixed dental prosthesis. J Adhes Sci Technol 2021;35:2529–2546.
15. Kaleli N, Ural Ç. Digital evaluation of laser scanning speed effects on the intaglio surface adaptation of laser-sintered metal frameworks. J Prosthet Dent 2020;123:874.e1–e7.
16. Di Angelo L, Di Stefano P, Guardiani E. Search for the optimal build direction in additive manufacturing technologies: A review. J Manuf Mater Process 2020;4:71.
17. Ekren O, Ozkomur A, Ucar Y. Effect of layered manufacturing techniques, alloy powders, and layer thickness on metal-ceramic bond strength. J Prosthet Dent 2018;119:481–487.
18. Koutsoukis T, Zinelis S, Eliades G, Al-Wazzan K, Rifaiy MA, Al Jabbari YS. Selective laser melting technique of Co-Cr dental alloys: A review of structure and properties and comparative analysis with other available techniques. J Prosthodont 2015;24:303–312.
19. Mazzoli A. Selective laser sintering in biomedical engineering. Med Biol Eng Comput 2013;51:245–256.
20. Ahmed N. Direct metal fabrication in rapid prototyping: A review. J Manuf Process 2019;42:167–191.
21. Ucar Y, Ekren O. Effect of layered manufacturing techniques, alloy powders, and layer thickness on mechanical properties of Co-Cr dental alloys. J Prosthet Dent 2018;120:762–770.
22. Örtorp A, Jönsson D, Mouhsen A, Vult von Steyern P. The fit of cobalt–chromium three-unit fixed dental prostheses fabricated with four different techniques: A comparative in vitro study. Dent Mater 2011;27:356–363.
23. Quante K, Ludwig K, Kern M. Marginal and internal fit of metal-ceramic crowns fabricated with a new laser melting technology. Dent Mater 2008;24:1311–1315.
24. Kim EH, Lee DH, Kwon SM, Kwon TY. A microcomputed tomography evaluation of the marginal fit of cobalt-chromium alloy copings fabricated by new manufacturing techniques and alloy systems. J Prosthet Dent 2017;117:393–399.
25. Ucar Y, Akova T, Akyil MS, Brantley WA. Internal fit evaluation of crowns prepared using a new dental crown fabrication technique: Laser-sintered Co-Cr crowns. J Prosthet Dent 2009;102:253–259.
26. Kulkarni P, Marsan A, Dutta D. A review of process planning techniques in layered manufacturing. Rapid Prototyp J 2000;6:18–35.
27. Alharbi N, Osman R, Wismeijer D. Effects of buid direction on the mechanical properties of 3D-printed complete coverage interim dental restorations. J Prosthet Dent 2016;115:760–767.
28. Allen S, Dutta D. On the computation of part orientation using support structures in layered manufacturing [Proceedings of the Solid Freeform Fabrication Symposium, Austin, TX, 1994]. University of Texas at Austin, 1994;259–269.
29. Dimitrov D, Schreve K, de Beer N. Advances in three dimensional printing—State of the art and future perspectives. Rapid Prototyp J 2006;12:136–147.

30. Puebla K, Arcaute K, Quintana R, Wicker RB. Effects of environmental conditions, aging, and build orientations on the mechanical properties of ASTM type I specimens manufactured via stereolithography. Rapid Prototyp J 2012;18:374–388.
31. Chaiamornsup P, Iwasaki N, Tsuchida Y, Takahashi H. Effects of build orientation on adaptation of casting patterns for three-unit partial fixed dental prostheses fabricated by using digital light projection. J Prosthet Dent 2022;128:1047–1054.
32. Ryu JE, Kim YL, Kong HJ, Chang HS, Jung JH. Marginal and internal fit of 3D printed provisional crowns according to build directions. J Adv Prosthodont 2020;12:225–232.
33. Osman B, Alharbi N, Wismeijer D. Build angle: Does it influence the accuracy of 3D-printed dental restorations using digital light-processing technology? Int J Prosthodont 2017;30:182–188.
34. Daou EE, Ounsi H, Özcan M, Al-Haj Husain N, Salameh Z. Marginal and internal fit of pre-sintered Co-Cr and zirconia 3-unit fixed dental prostheses as measured using microcomputed tomography. J Prosthet Dent 2018;120:409–414.
35. Gu D, Shen Y. Balling phenomena in direct laser sintering of stainless steel powder: Metallurgical mechanisms and control methods. Mater Des 2009;30:2903–2910.
36. BEGO Implant Systems. Mediloy S-Co. The non-precious allow for the production of dental restorations. Accessed 14 November 2023. https://www.bego.com/cad-cam-solutions/materials/non-precious-metal-alloys/mediloy-s-co/
37. Kaleli N, Ural Ç, Özköylü G, Duran İ. Effect of layer thickness on the marginal and internal adaptation of laser-sintered metal frameworks. J Prosthet Dent 2019;121:922–928.
38. Tsitrou EA, Northeast SE, van Noort R. Evaluation of the marginal fit of three margin designs of resin composite crowns using CAD/CAM. J Dent 2007;35:68–73.
39. Park GS, Kim SK, Heo SJ, Koak JY, Seo DG. Effects of printing parameters on the fit of implant-supported 3D printing resin prosthetics. Materials (Basel) 2019;12:2533.
40. Alharbi N, Osman R, Wismeijer D. Factors influencing the dimensional accuracy of 3D-printed full-coverage dental restorations using stereolithography technology. Int J Prosthodont 2016;29:503–510.
41. Chaiamornsup P, Iwasaki N, Yasue T, Uo M, Takahashi H. Effects of build conditions and angle acuteness on edge reproducibility of casting patterns fabricated using digital light projection. Dent Mater J 2020;39:135–140.
42. Unkovskiy A, Bui PHB, Schille C, Geis-Gerstorfer J, Huettig F, Spintzyk S. Objects build orientation, positioning, and curing influence dimensional accuracy and flexural properties of stereolithographically printed resin. Dent Mater 2018;34:e324–e333.
43. Daou EE. Effect of lamination layer thickness and abutment preparation on the fit of Co-Cr multi-unit prostheses fabricated by additive manufacturing: An in vitro study. J Prosthet Dent 2022. Epub ahead of print.
44. Paul R, Anand S. Optimization of layered manufacturing process for reducing form errors with minimal support structures. J Manuf Syst 2015;36:231–243.
45. Pandey PM, Reddy NV, Dhande SG. Slicing procedures in layered manufacturing: A review. Rapid Prototyp J 2003;9:274–288.
46. Revilla-León M, Al-Haj Husain N, Methani MM, Özcan M. Chemical composition, surface roughness, and ceramic bond strength of additively manufactured cobalt-chromium dental alloys. J Prosth Dent 2021;125:825–831.
47. Gu D, Shi Q, Lin K, Xi L. Microstructure and performance evolution and underlying thermal mechanisms of Ni-based parts fabricated by selective laser melting. Addit Manuf 2018;22:265–278.
48. Davoodi E, Montazerian H, Mirhakimi AS, et al. Additively manufactured metallic biomaterials. Bioact Mater 2022;15:214–249.
49. Maconachie T, Leary M, Lozanovski B, et al. SLM lattice structures: Properties, performance, applications and challenges. Mater Des 2019;183:108137.
50. Masood SH, Rattanawong W, Iovenitti P. Part build orientations based on volumetric error in fused deposition modelling. Int J Adv Manuf Technol 2000;16:162–168.
51. Xin XZ, Chen J, Xiang N, Wei B. Surface properties and corrosion behavior of Co-Cr alloy fabricated with selective laser melting technique. Cell Biochem Biophys 2013;67:983–990.
52. Vandenbroucke B, Kruth JP. Selective laser melting of biocompatible metals for rapid manufacturing of medical parts. Rapid Prototyp J 2007;13:196–203.
53. Wu S, Brown D, Kumar M, Gallegos GF, King W. An experimental investigation into additive manufacturing–induced residual stresses in 316L stainless steel. Metall Mater Trans A 2014;45:6260–6270.
54. Huang Z, Zhang L, Zhu J, Zhang X. Clinical marginal and internal fit of metal ceramic crowns fabricated with a selective laser melting technology. J Prosthet Dent 2015;113:623–627.
55. Kaleli N, Ural Ç, Ölçer Us Y. Evaluation of marginal discrepancy in metal frameworks fabricated by sintering-based computer-aided manufacturing methods. J Adv Prosthodont 2020;12:124–130.
56. Belser U, MacEntee MI, Richter WA. Fit of three porcelain-fused-to-metal marginal designs in vivo: A scanning electron microscope study. J Prosthet Dent 1985;53:24–29.
57. Beuer F, Aggstaller H, Edelhoff D, Gernet W, Sorensen J. Marginal and internal fits of fixed dental prostheses zirconia retainers. Dent Mater 2009;25:94–102.
58. Nakamura T, Dei N, Kojima T, Wakabayashi K. Marginal and internal fit of Cerec 3 CAD/CAM all-ceramic crowns. Int J Prosthodont 2003;16:244–248.
59. Scherrer SS, de Rijk WG, Belser UC, Meyer JM. Effect of cement film thickness on the fracture resistance of a machinable glass-ceramic Dent Mater 1994;10:172–177.
60. Kokubo Y, Ohkubo C, Tsumita M, Miyashita A, Vult von Steyern P, Fukushima S. Clinical marginal and internal gaps of Procera AllCeram crowns. J Oral Rehabil 2005;32:526–530.
61. Alharbi N, Alharbi S, Cuijpers VMJI, Osman RB, Wismeijer D. Three-dimensional evaluation of marginal and internal fit of 3D-printed interim restorations fabricated on different finish line designs. J Prosthodont Res 2018;62:218–216.
62. Cheng W, Fuh FYH, Nee AYC, Wong YS, Loh HT, Miyazawa T. Multi-objective optimization of part- building orientation in stereolithography. Rapid Prototyp J 1995;1:12–23.
63. Chowdhury S, Mhapsekar K, Anand S. Part build orientation optimization and neural network–based geometry compensation for additive manufacturing process. J Manuf Sci Eng 2018;140:031009.